Supporting Information (SI)

Extending the scope of a new cyanation: Design and synthesis of an anthracene derivative with exceptionally low LUMO level and improved solubility

Florian Glöcklhofer,*[†] Andreas J. Morawietz,[†] Berthold Stöger,[‡] Miriam M. Unterlass[§] and Johannes Fröhlich[†]

[†]*Institute of Applied Synthetic Chemistry, TU Wien, Getreidemarkt 9/163, 1060 Vienna, Austria.*

[‡]*Institute of Chemical Technologies and Analytics, TU Wien, Getreidemarkt 9/164, 1060 Vienna, Austria.*

[§]*Institute of Materials Chemistry, TU Wien, Getreidemarkt 9/165, 1060 Vienna, Austria.*

E-Mail: florian.gloecklhofer@tuwien.ac.at

Table of contents:

1. ^{1}H-, ^{13}C(APT)-NMR spectra

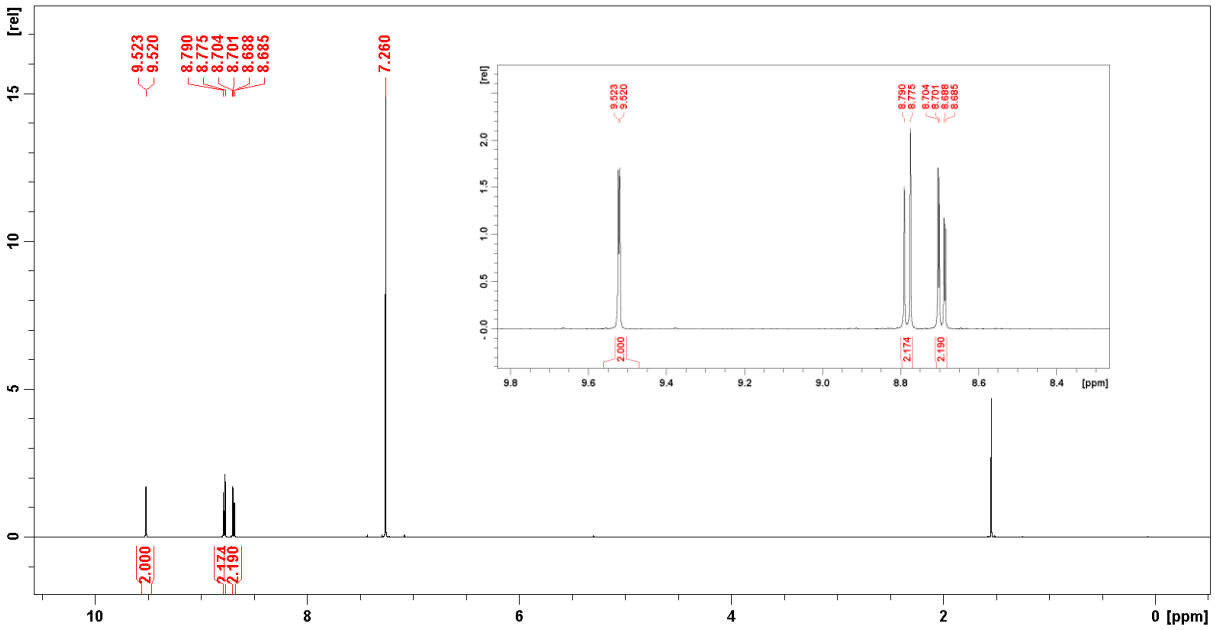

Figure S1: ^{1}H NMR spectrum (600 MHz, $CDCl_3$) of **2**.

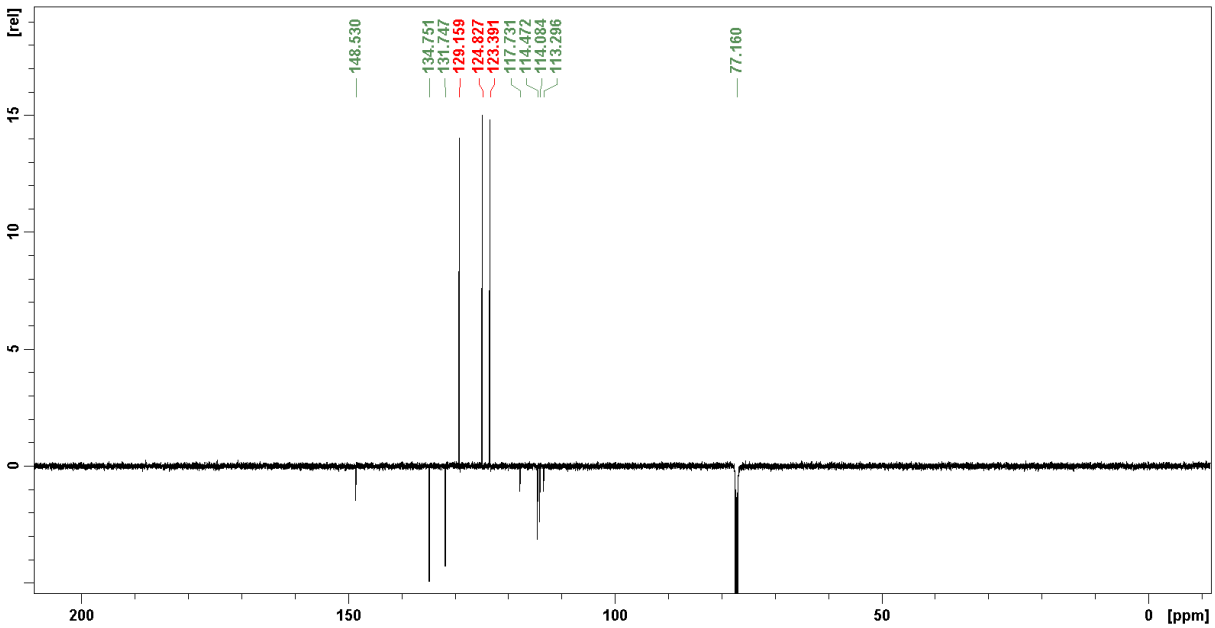

Figure S2: ^{13}C NMR spectrum (150 MHz, $CDCl_3$) of **2**.

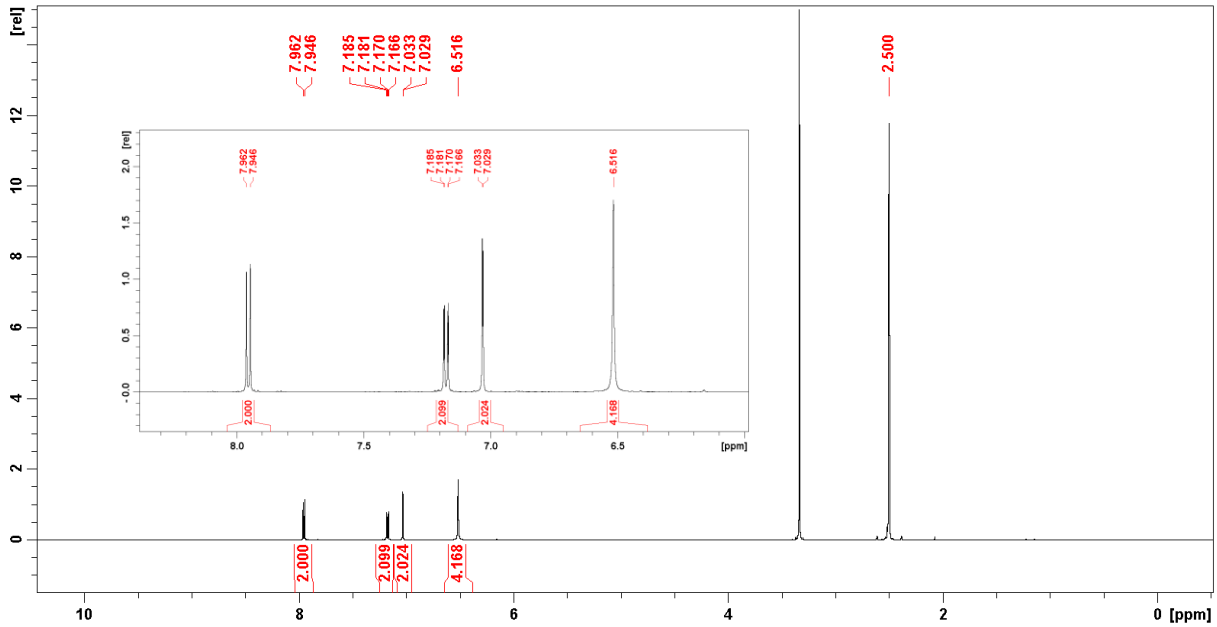

Figure S3: ^{1}H NMR spectrum (600 MHz, DMSO-d_6) of **3**.

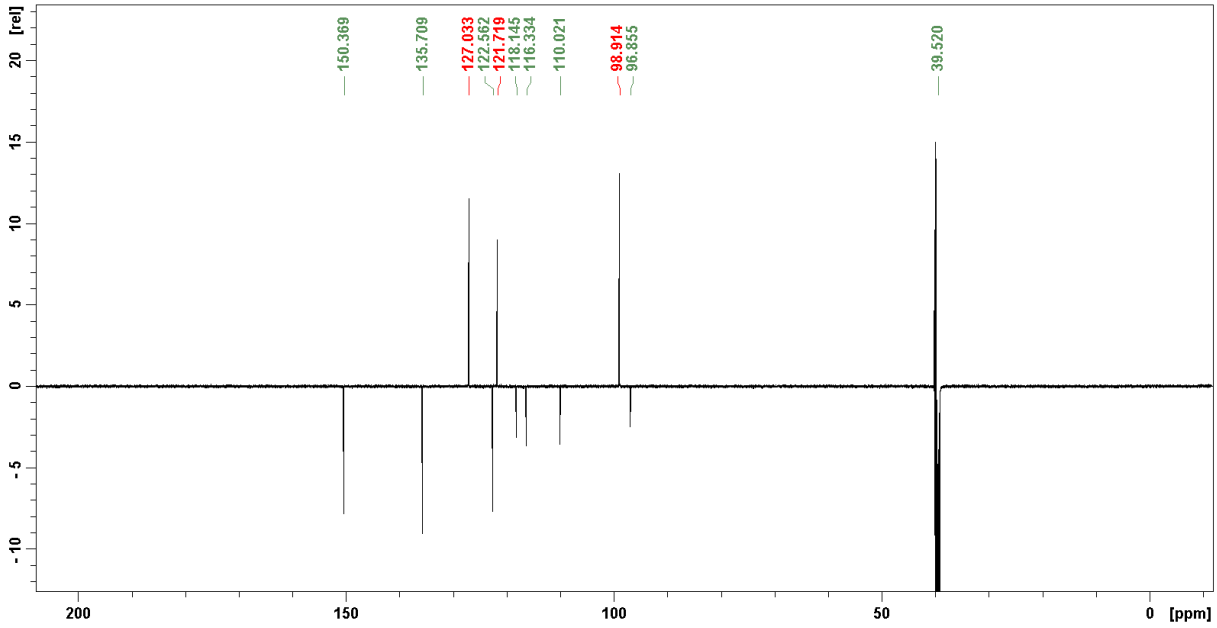

Figure S4: ^{13}C NMR spectrum (150 MHz, DMSO-d_6) of **3**.

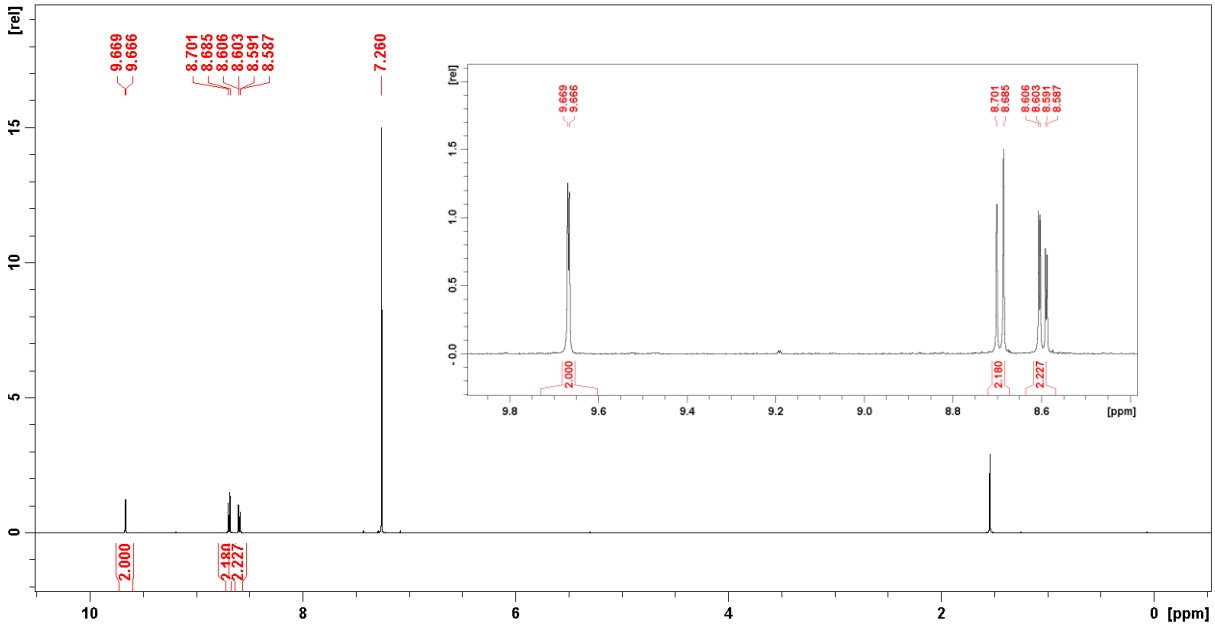

Figure S5: ^{1}H NMR spectrum (600 MHz, $CDCl_3$) of **4**.

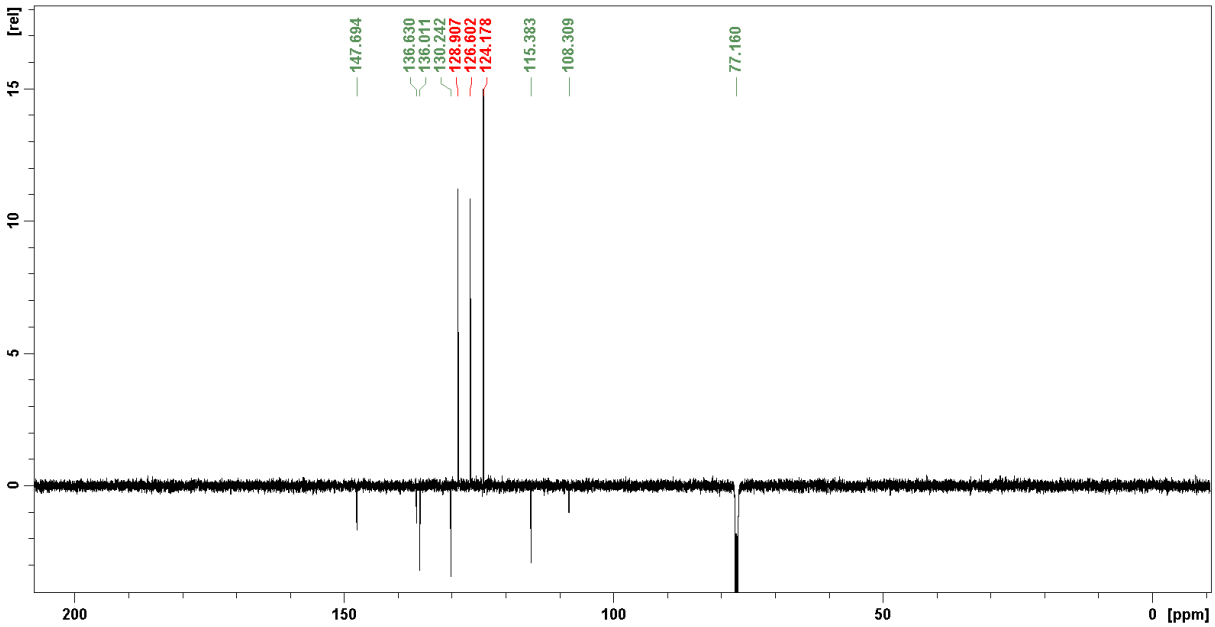

Figure S6: ^{13}C NMR spectrum (150 MHz, $CDCl_3$) of **4**.

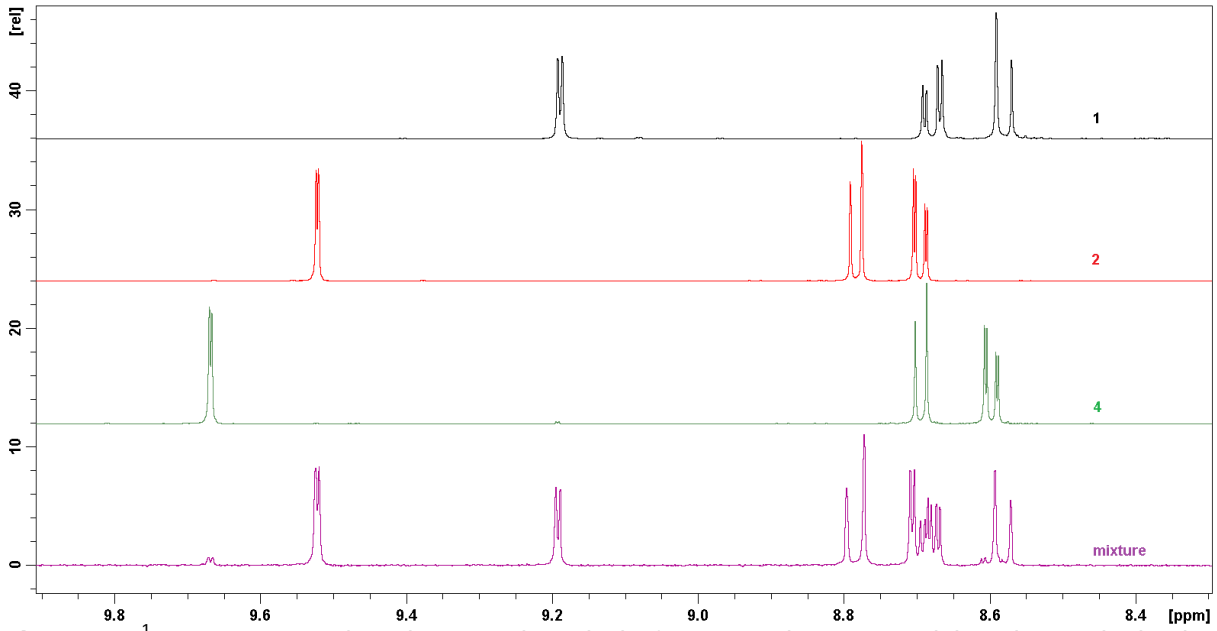

Figure S7: ^{1}H NMR spectra ($CDCl_3$, aromatic region) of compounds **1**, **2**, **4** and the mixture obtained as byproduct in the synthesis of **4**.

2. Cyclic voltammetry (CV)

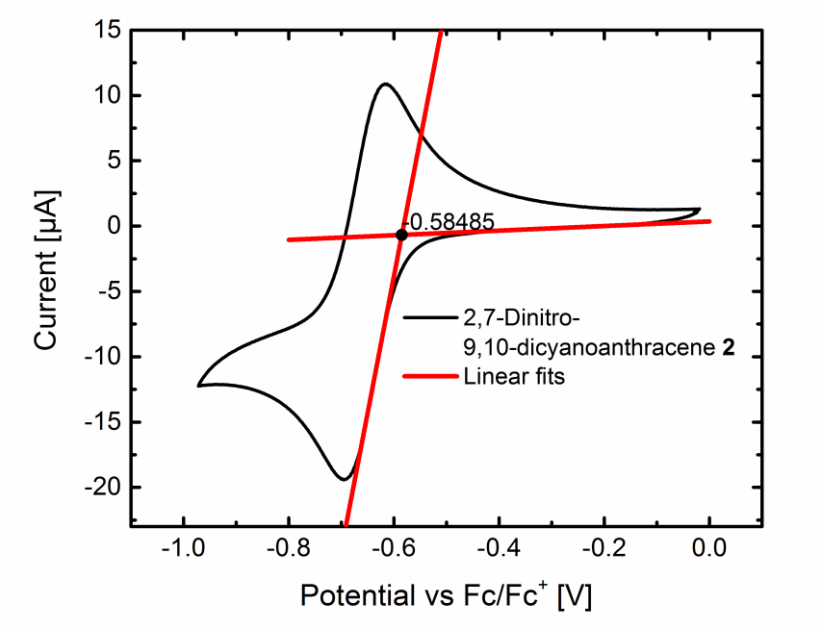

Figure S8: Cyclic voltammogram of **2** in acetonitrile solution; reduction onset at -0.58 V corresponds to a LUMO level of -4.22 eV.

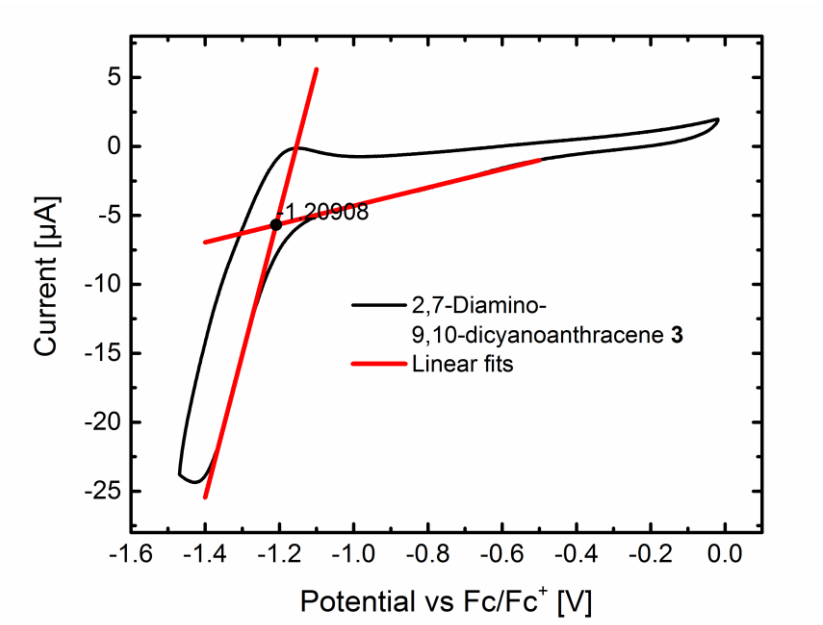

Figure S9: Cyclic voltammogram of **3** in acetonitrile solution; reduction onset at -1.21 V corresponds to a LUMO level of -3.59 eV.

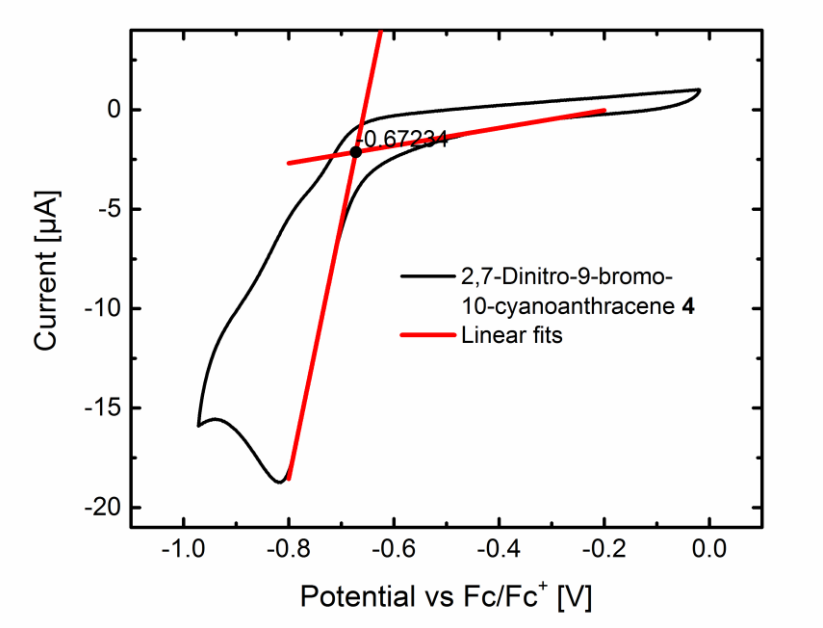

Figure S10: Cyclic voltammogram of **4** in acetonitrile solution; reduction onset at -0.67 V corresponds to a LUMO level of -4.13 eV.

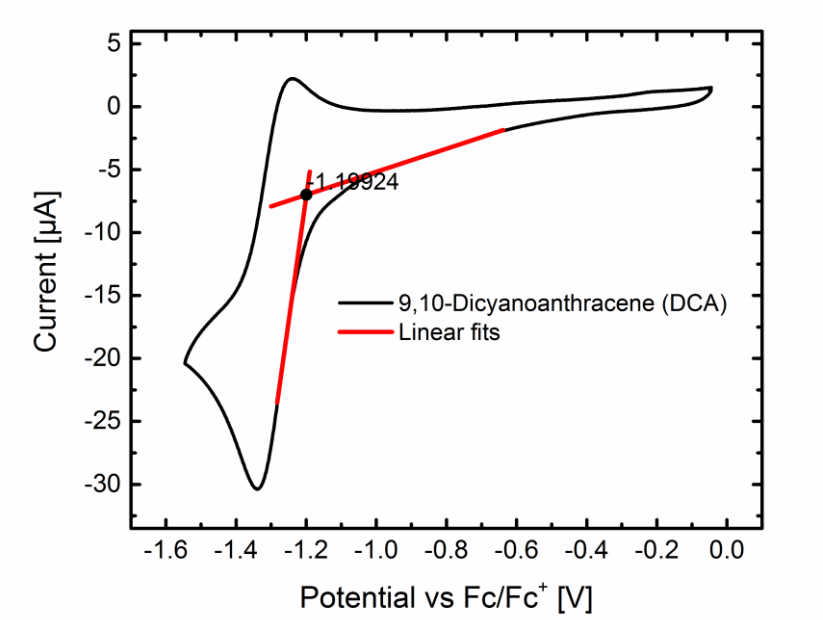

Figure S11: Cyclic voltammogram of 9,10-dicyanoanthracene (DCA) in acetonitrile solution; reduction onset at -1.20 V corresponds to a LUMO level of -3.60 eV.

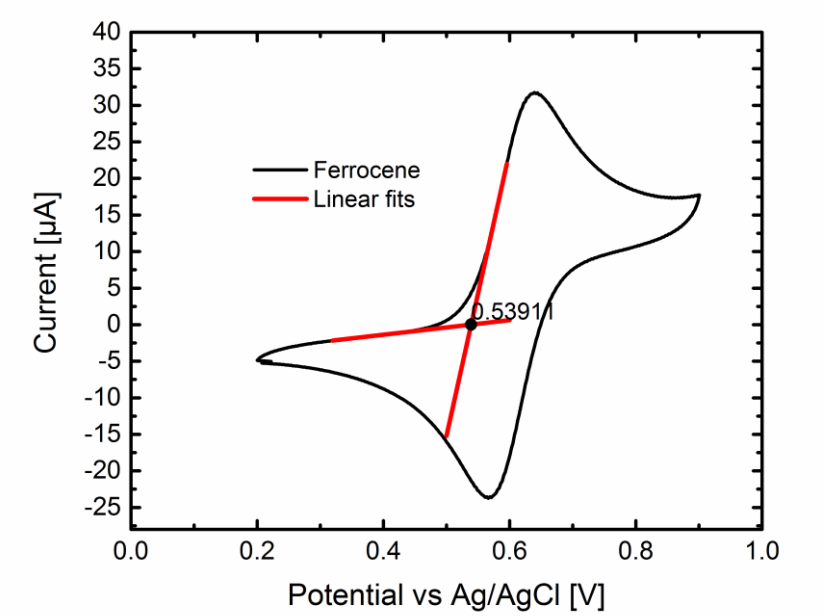

Figure S12: Reference measurement of ferrocene in acetonitrile solution; oxidation onset at 0.54 V.

3. UV-Vis absorption

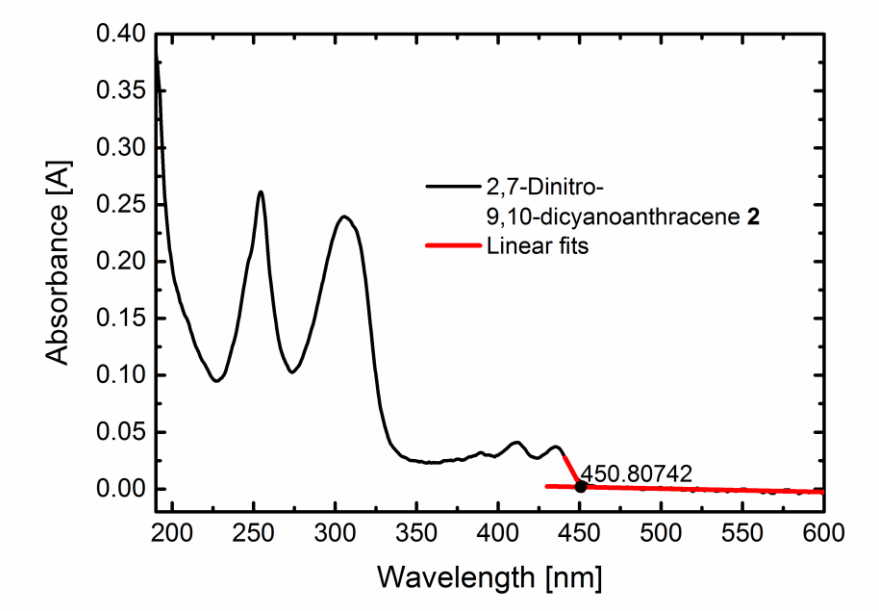

Figure S13: UV-vis absorption spectrum of **2** in acetonitrile solution; absorption onset at 450.81 nm corresponds to an optical bandgap of 2.75 eV.

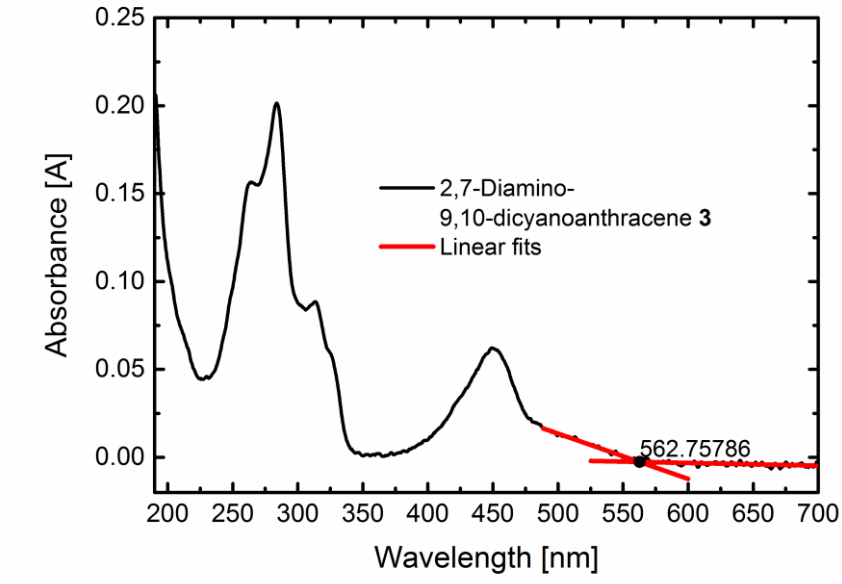

Figure S14: UV-vis absorption spectrum of **3** in acetonitrile solution; absorption onset at 562.76 nm corresponds to an optical bandgap of 2.20 eV.

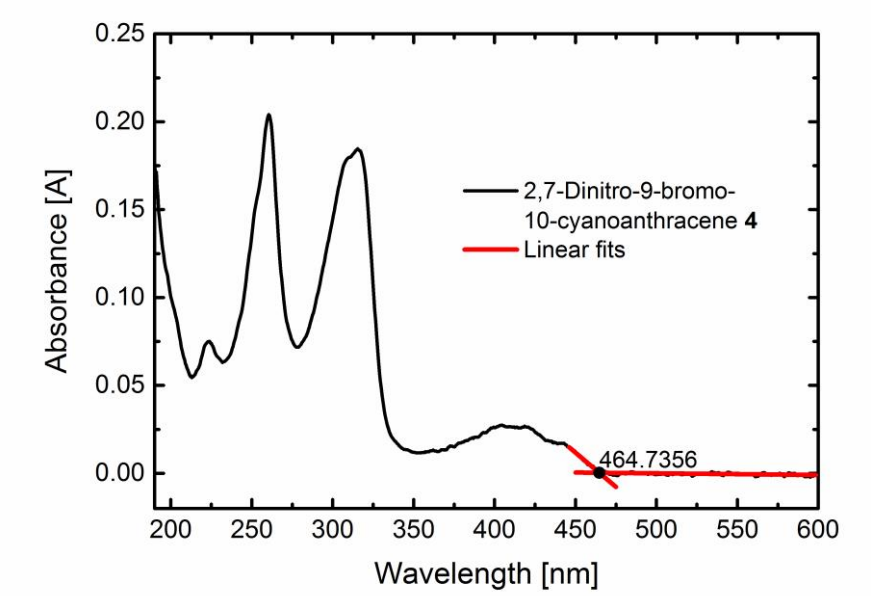

Figure S15: UV-vis absorption spectrum of **4** in acetonitrile solution; absorption onset at 464.74 nm corresponds to an optical bandgap of 2.67 eV.

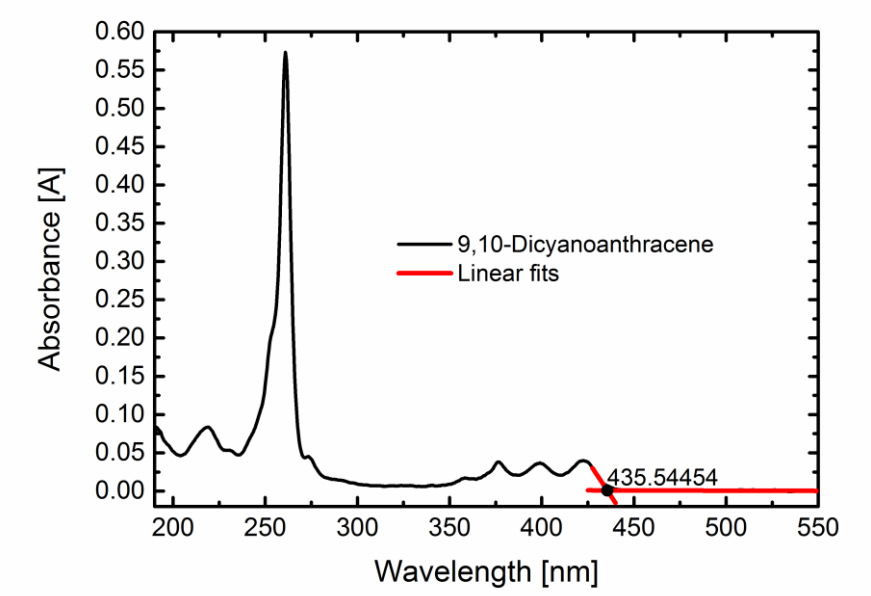

Figure S16: UV-vis absorption spectrum of 9,10-dicyanoanthracene (DCA) in acetonitrile solution; absorption onset at 435.54 nm corresponds to an optical bandgap of 2.85 eV.

4. Fluorescence emission

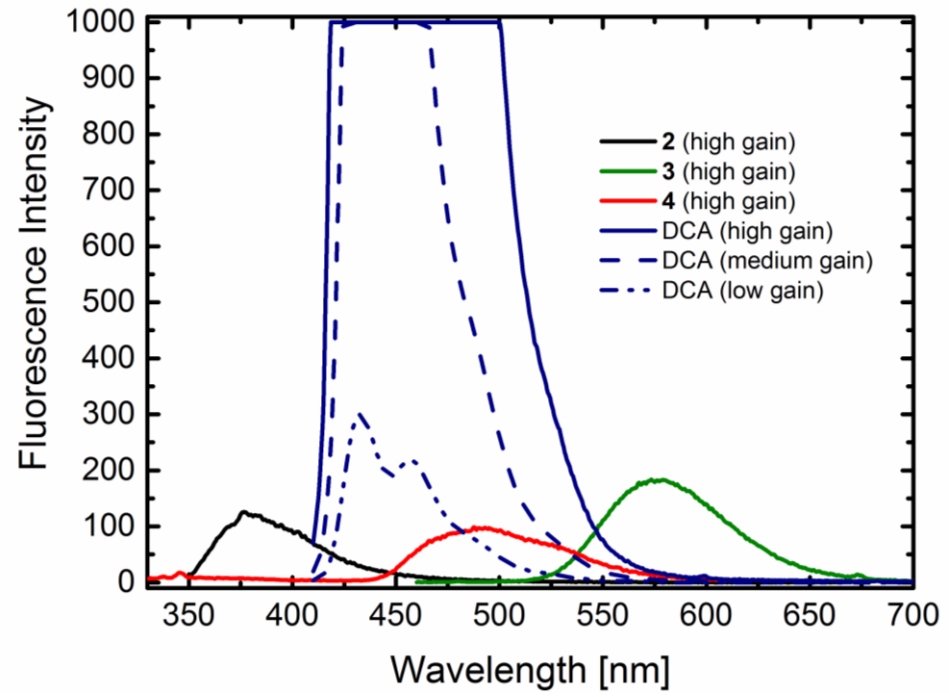

Figure S17: Fluorescence emission spectra of **2**, **3**, **4**, and DCA in acetonitrile solution. Excitation wavelengths: 340 nm (**2**), 450 nm (**3**), 315 nm (**4**); 400 nm (DCA).

5. Thermogravimetric analysis (TGA)

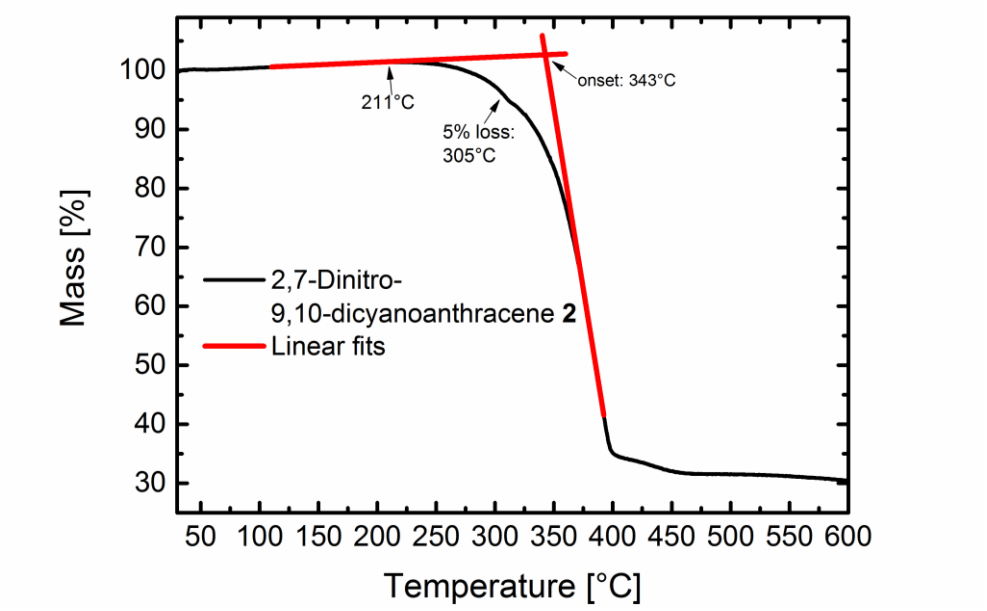

Figure S18: Thermogravimetric analysis of **2**.

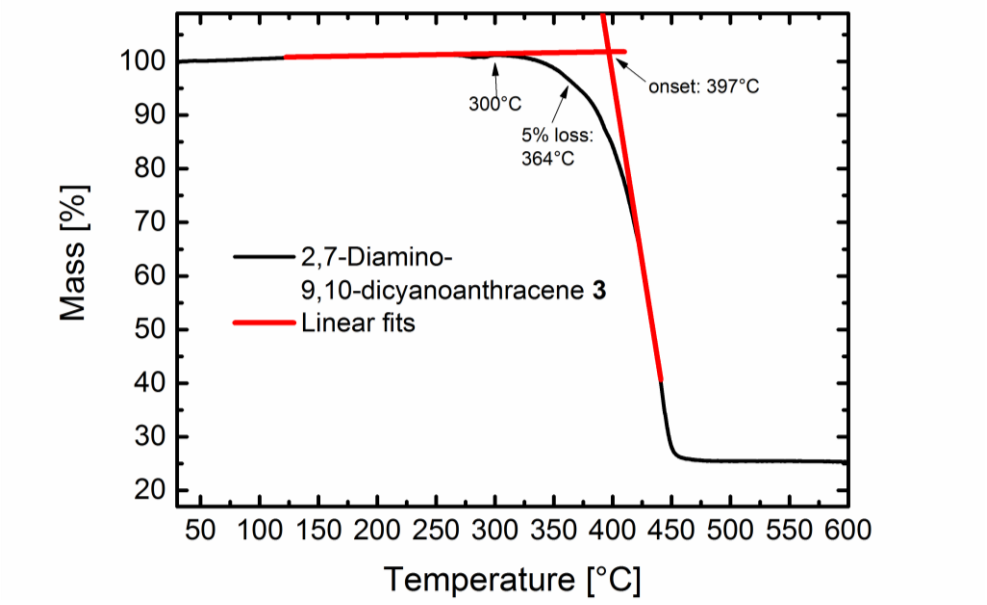

Figure S19: Thermogravimetric analysis of **3**.

6. X-ray structure determination

Table S1. Details for the crystal structure determinations of **2** and **4**.

	2	**4**
formula	$C_{16}H_6N_4O_4$	$C_{15}H_6BrN_3O_4$
fw	318.2	372.1
cryst.size, mm	0.54 x 0.21 x 0.04	0.48 x 0.46 x 0.05
color, shape	yellow, needle-like	yellow, plate
crystal system	monoclinic	monoclinic
space group	$P2_1$ (no. 4)	$P2_1/c$ (no. 14)
a, Å	3.7419(4)	7.4784(11)
b, Å	8.4966(9)	8.6549(12)
c, Å	20.448(2)	20.629(3)
β, °	90.597(3)	94.493(4)
V, Å^3	650.06(12)	1331.1(3)
T, K	100	100
Z, Z'	2, 1	4, 1
ρ_{calc}, g cm^{-3}	1.6259	1.857
μ, mm^{-1} (MoKα)	0.122	3.115
F(000)	324	736
absorption corrections	multi-scan	multi-scan
T_{min}-T_{max}	0.94–1.00	0.22–0.86
θ range, deg	1.00–30.12	1.98–35.03
no. of rflns measd	9571	34605
R_{int}	0.0314	0.0400
no. of rflns unique	3787	5861
no. of rflns $I>3\sigma(I)$	3218	4629
no. of params / restraints	217 / 0	208 / 0
R ($I > 3\sigma(I)$) [a]	0.0464	0.0289
R (all data)	0.0563	0.0446
wR ($I > 3\sigma(I)$)	0.0697	0.0392
wR (all data)	0.0725	0.0420
GooF	1.54	1.30
Diff.Four.peaks min/max, eÅ^{-3}	-0.22 / 0.34	-0.67 / 1.01
CCDC no.	1530990	1530991

[a] $R = \Sigma||F_o|-|F_c|| / \Sigma|F_o|$, $wR = \Sigma w(|F_o| - |F_c|) / \Sigma w|F_o|$, GooF = $\{\Sigma[w(F_o^2 - F_c^2)^2] / (n-p)\}^{½}$

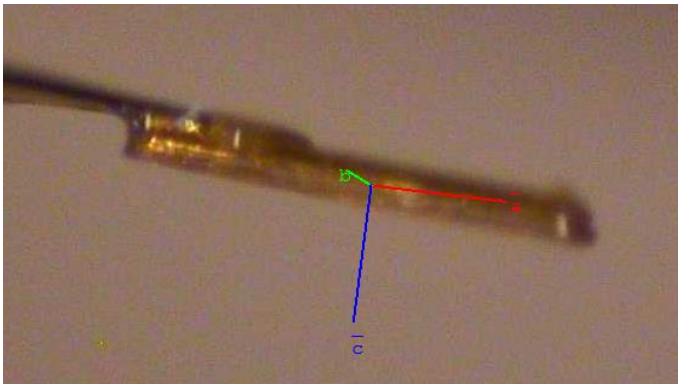

Figure S20: Orientation of **2** in the diffractometer.

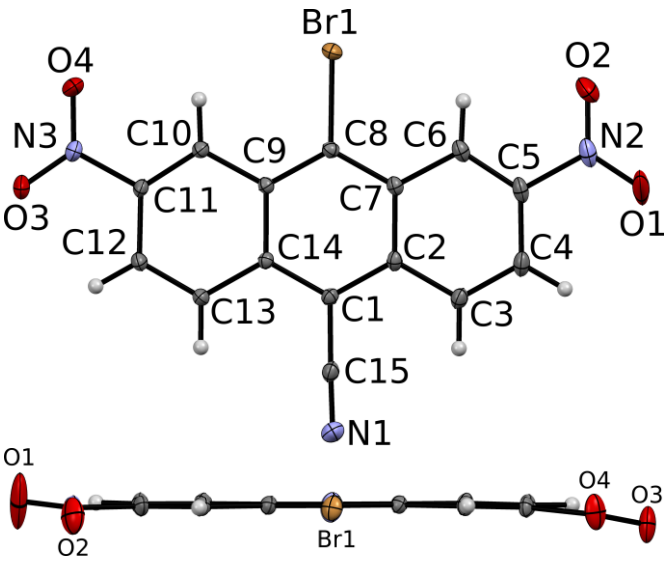

Figure S21: Molecular structure of **4**. Ellipsoids drawn at the 50% probability levels, H atoms represented by white spheres of arbitrary radius.

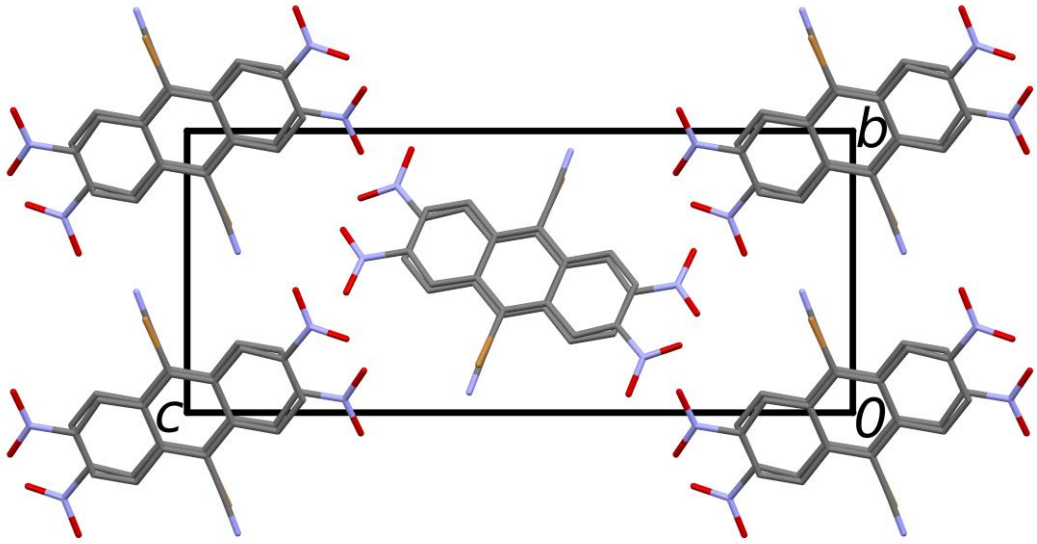

Figure S22: Crystal structure of **4**. Colors as in Figure S19; H atoms were omitted for clarity.

7. High-performance liquid chromatography (HPLC) measurements

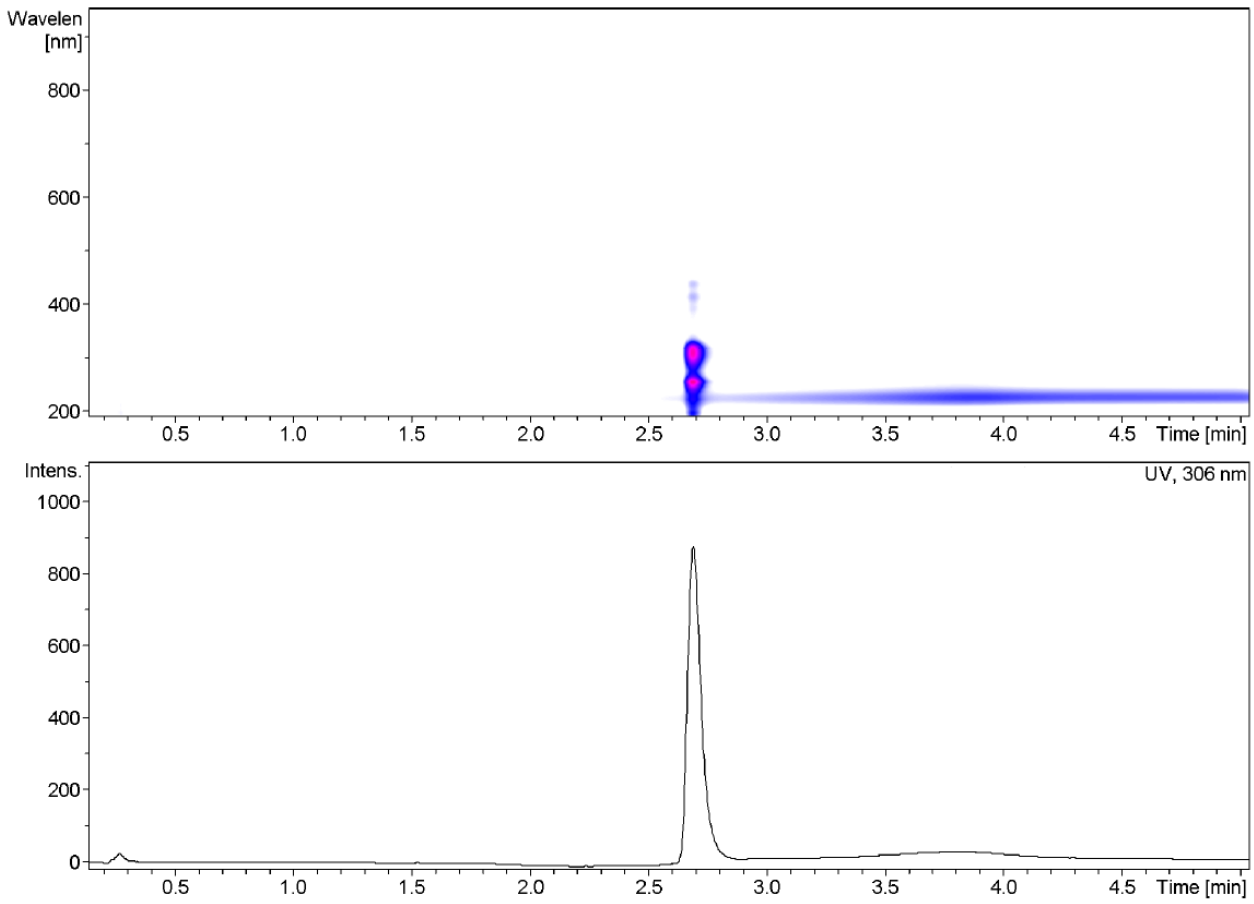

Figure S23: Chromatogram of **2** (sample dissolved in acetonitrile). The signal starting at 3.0 min is caused by high concentrations of acetonitrile in the mobile phase.

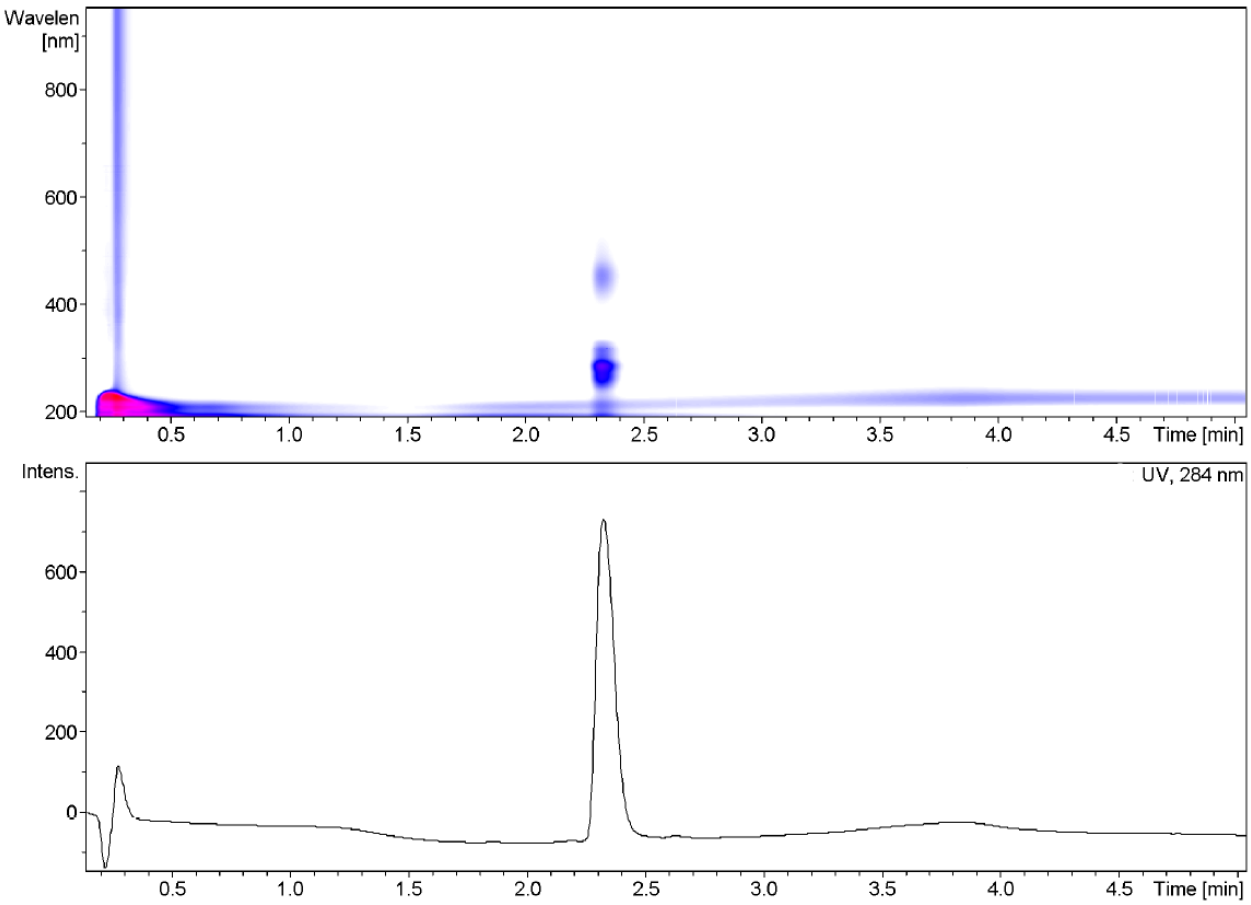

Figure S24: Chromatogram of **3** (sample dissolved in DMSO). The signal starting at 3.0 min is caused by high concentrations of acetonitrile in the mobile phase.

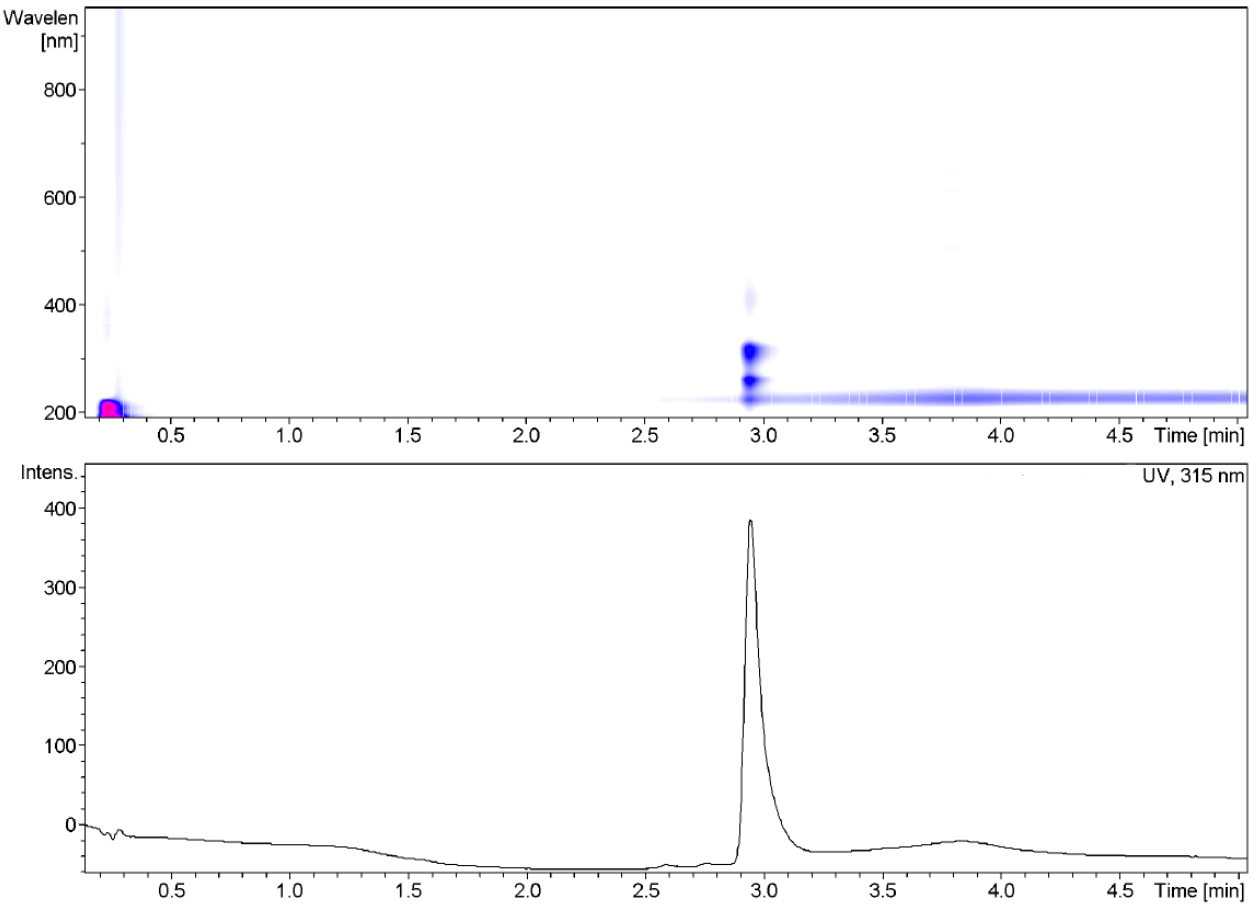

Figure S25: Chromatogram of **4** (sample dissolved in acetonitrile). The signal starting at 3.0 min is caused by high concentrations of acetonitrile in the mobile phase.